Observational Study of Landslide Mechanism in the Area of Crystalline Schist (Part 2)

—An Application of 2-D F. E. M. —

By Akira SUEMINE

(Manuscript received March 9, 1987)

Abstract

In order to explain the behavior of landsliding observed in an area of crystalline schist in September 1980, numerical simulation has been conducted by the finite element method under the effects of self-weight and five different pore-water pressures; corresponding to 0.25, 0.5, 0.75, 1.0 or 1.25 times the observed groundwater level. The finite element method is supplemented by joint elements as introduced by Goodman. The joint elements are so devised to express the shear stress to follow the Mohr-Coulomb's failure criterion and the normal stress not to be transmitted across a joint once the joint element has been opened by the tensile stress. The joint elements are arranged along the slip surface determined by measurements using the pipe strain-meters and an insert type of strain meter. The soil above the slip surface is assumed to be linearly elastic. By the initial position and the progression direction of rupture, crystalline-schist landslides can be classified into 3 types. This simulation explains a case where the rupture starts at a point in the slope and progresses downwards at an average velocity of a few meters per hour. It is pointed out that the progression of the rupture has been controlled essentially by rise and fall of the pore-water pressure accompanied by rainfall during the slide.

1. Introduction

Behaviors of landslides have been monitored by means of a variety of instruments up to the present. The main purposes of such monitoring have been to determine landslide features such as landslide boundary, the depth of slip surface, the compression and extension regions, the landslide direction and the displacement magnitude, to predict landslide occurrence time, and to find out effective countermeasures. We also have observed a number of crystalline-schist landslides in the Island of Shikoku, Japan. Through the observations, we have aimed at the elucidation of not only the landslide features etc. mentioned above but also the landslide mechanism. In order to prevent a natural or an artificial landslide, an understanding of landslide mechanism would greatly help us to decide the place and dimension of an effective countermeasure because a countermeasure at the landslide-initiation point could be most economical in preventing the slide.

The author explains the landslide mechanism, which is considered in this paper, using **Fig. 1.** The landslide-nucleation position as the starting point of rupture, the direction and the velocity of rupture progression along the slip surface (V) and the
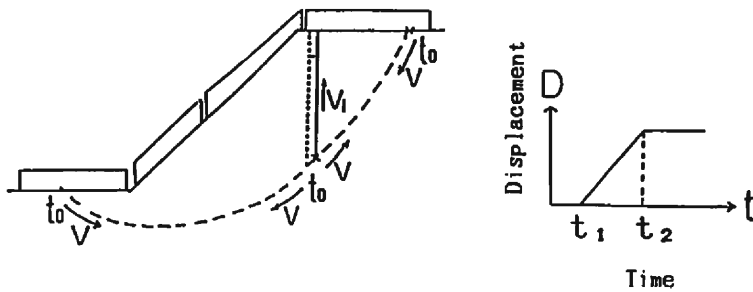
Fig. 1. Model of landslide mechanism. t_0 is the time of rupture initiation. t_1 and t_2 are the times of the initiation and stopping of displacement at a point, respectively. V_1 and V are the rupture velocities along the vertical and lateral directions, respectively. D is the magnitude of displacement and $T = t_2 - t_1$ is rise time. The extensometer are set up on the ground surface to observe the ground-surface strain. The pipe strain-meters are installed for observing the differential displacement within the earth.

velocity of rupture propagation from slip surface to the ground surface (V_1) are shown in the left inset of the figure. The subsurface-displacement and the surface-displacement velocity which is calculated as D/T from displacement D and the rise time T, are shown in the right of the figure. A related question is whether the magnitude and time history of the displacement are function of the place or not.

In the previous papers[1],[2] the author described the landslide mechanism based on a series of observations at crystalline-schist landslides. The results may be summarized as follows. By the initiation position and the progression direction of the rupture, which are two of the important physical characteristics of the landslide mechanism, the landslide can be classified into 3 types. The first type is characterized by the rupture starting at the lower part of the slope and progressing to the upper part at an average velocity from a few meters per hour to about 10 meters per hour ; the second type by the rupture starting in the middle of the slope and progressing bilaterally along the slope at an average velocity of a few meters per hour ; and the third type by the rupture starting at the upper part of the slope and progressing downwards at an average velocity of a few meters per hour.

Slip surfaces were determined through observation of strains within the ground using pipe strain-meters (internal strain meters) and an insert type of strain meter[3] at 44 boring sites in four crystalline-schist landslides investigated by us in Shikoku. The pipe strain-meter is an instrument where strain gauges are attached to a vinyl chloride pipe. Thirty-seven of these observed sites revealed that there was only one slip surface in each landslide. This figure is equivalent to 84 percent of the total observed slip surfaces. In 7 remaining sites, where two slip surfaces in a borehole were suspected by means of the pipe strain-meters, the deeper slip surface could not be confirmed with the insert type of strain meter because the boreholes were cut off by the shallower slip surfaces and deeper insertion was not possible. Therefore some of the deeper slip surfaces anticipated at these 7 sites may be observational errors. Consequently, many landslides in crystalline schist in Shikoku have very likely only one slip surface. In addition, the

observations utilizing the pipe and the insert type of strain meter also indicated that the landslide movement in many cases could occur along the same slip surface almost every year[4].

This paper will present a theoretical explanation of the phenomena where in the rupture starts at a point in the slope and progresses downwards at an average velocity of a few meters per hour, by using the finite element method (F. E. M.). First, a brief history in the stability analysis is described and the inadequacy of the stability analysis in elucidating the landslide mechanism is pointed out, and the F. E. M. as a more appropriate means is introduced. Second, the special features of the finite element method used in this paper is described. Third, the results of an application of this method to a crystalline-schist landslide are presented and discussed to give a theoretical implication of the observed landslide process.

2. Stability Analysis and Finite Element Method

Stability analysis of slopes has been conducted for a long time. For example, the circular arc method was proposed in Sweden in the beginning of this century. Fllenius developed a method for calculating a factor of safety, including cohesion and internal friction angle, and this method was popularized in the 1930s as the Swedish method[5]. Morgenstern and Price[6], and Spencer[7] developed the works done by Taylor, Janbu[8] and Bishop[9] to form a theoretical equation for a factor of safety of general slip surfaces based on the slice method.

The first introduction of the method into Japan was made by N. Yamaguchi in 1934 and by Z. Anzou in 1940 in the form of the mathematical equations and diagrams of the circular arc method. The theoretical equations based on the slice method of circular slip surface and non-circular slip surface were derived by T. Nomitsu in 1942[10]. In this case the internal forces of the general slip surface were assumed to be parallel to the ground surface.

In the general slice methods, where limit-equilibrium condition is assumed, strains and statically-indeterminate stresses are not dealt with explicitly. Therefore the stability factor for each slice is not calculated explicitly. Thus, the methods are incapable of giving probable stresses on the slip surface which are essential for the use of failure criterion.

The use of F. E. M. can eliminate this difficulty accompanying the general slice method under the limit-equilibrium condition ; the shape of slip surface, the determination of internal stress or the direction of resultant internal force. The stress and strain in the ground can be rationally calculated by using F. E. M., therefore the normal stress and shear stress at each and every point along the slip surface can be obtained. Assumptions with regards to statically-indeterminate stresses become unnecessary. A local as well as total factor of safety also can be calculated more reliably by using F. E. M. In this respect, the F. E. M. is superior to conventional stability analysis.

The analysis of the progressive failure by using F. E. M. with Haefelis's residual-coefficient concept was first conducted by Kitahara[11] for slope stability during excavation.

Lo et al[12]. have also analyzed the landslide of progressive-failure type by F. E. M. In these studies of progressive failure of a given slope, they generally treated a slope's stability over a long term, where strength along the slip surface decreases gradually with infiltration of water canceling out the negative pore pressure. In these applications of the F. E. M., progressive failure was denoted by the shear failure zones of triangular elements, however the actual slip surface is more or less 10 centimeters thick. Consequently, these F. E. M. analyses do not strictly show the actual landslide movement. Recently, stability analysis of dams et al. by F. E. M. using the Kawai model (Rigid-Body and Spring Model) have been reported by Hada et al[13].

However, a limited number of analyses of safety factor and deformation conditions of slope by F. E. M. have been carried out until the present as summarized above. Furthermore, a comparison of the observed results with calculated results for the landslide mechanism during local heavy rainfall or typhoon, when groundwater level rose, has not been conducted at all as far as the author is aware. The reason for this situation may be partly due to the fact that very few spatial-temporal continuous and quatitative observations or landslide movements have been made so far, and the data which are prerequisite for the analysis have not been available. The observation conducted by the author in his previous paper[1] made it possible to apply the F. E. M. to landsliding by a heavy rainfall for analyzing that process quantitatively.

3. Model and Analyzed Cases of Landslide in the Present Study

3. 1 The Irahara Landslide

The landslide area chosen for the present analysis is Irahara[14], Tokushima Prefecture in Shikoku, where typical physical constants of soil are available. The P-wave profile was determined by seismic survey conducted in Irahara[14]. Density, cohesion and internal friction angle have been determined by soil test including triaxialtests under $\overline{CU}$ condition for core samples obtained from boreholes[15]. Geological and topographic details of this area have been given in the previous paper[1]. **Figure 2** shows the arrangement of instruments in the landslide area. The numbers assigned to internal strain meters in the previous paper[1] are changed in this paper. The table of correspondence is given in the Appendix.

The main physical characteristics (rupture-progression velocity and the initiation position of the rupture along the slip surface) were determined through the observations in situ during the actual landslide caused by a rainfall of more than 570 millimeters in a few days in September 1980. Measurements were made with respect to line A in **Fig. 2** by the pipe strain-meters, tiltmeters, extensometers and piezometers. Boreholes were simultaneously employed as pipe strain-meters and piezometers at that time. The observations of tiltmeters and extensometers showed that the whole landslide block, where the pipe strain-meters (A5, A6) had been installed, moved at that time. The velocity of progression of the rupture along a slip surface is calculated from the distance between the pipe strain-meters divided by the time difference of rupture outbreaks or breakage of the pipe strain-meters. Rupture was found to have occurred
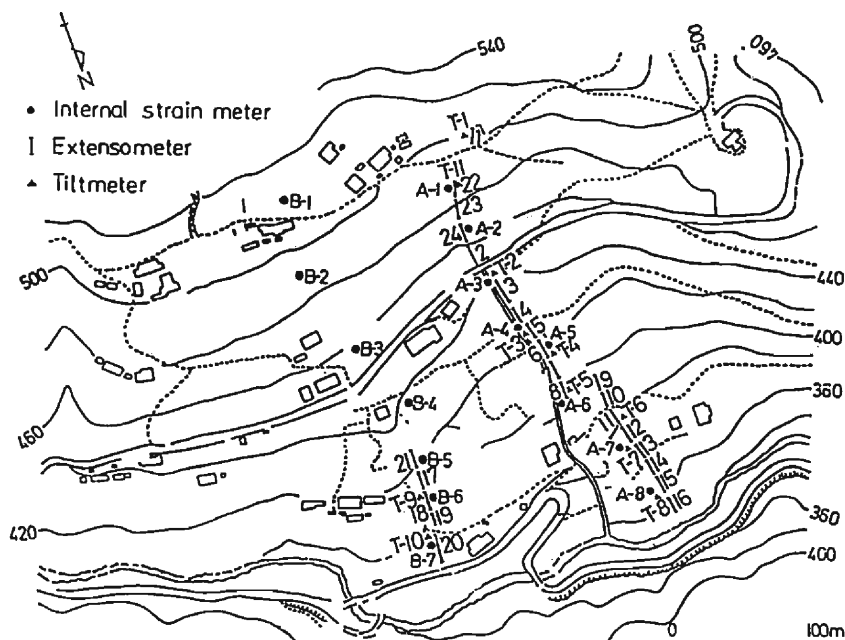
Fig. 2. Arrangement of instruments at the Irahara landslide area. A-m or B-n denotes the pipe strain-meter. T-1 denotes the tiltmeter.

Table 1. List of the rupture velocity along line A; The strain rate was evaluated as the change during one minute just after the onset time

	Onset time	Variation of strain	Rupture Progression-velocity
A 5 7.5m	17.18 9/10/80	-63×10^{-6}	
A 6 6.5m	07.47 9/11/80	-24×10^{-6}	2.5m/hour
A 5 7.5m	08.17 9/11/80	1599×10^{-6}	
A 6 6.5m	04.23 9/12/80	-1391×10^{-6}	1.8m/hour
A 5 7.5m	16.51 9/11/80	scale over	
A 6 6.5m	11.27 9/12/80	scale over	2.2m/hour

at the slip surface near the pipe strain-meter A5. The rupture progressed downward to A6 at a speed averaging a few meters per hour (see **Table 1**)[1]. The groundwater level during the landslide movement was measured once a day[15].

Figure 3 shows some of the results of the observations made by the insert type of strain meter on the targeted area. The accuracy of the measurement is approximately 200 microstrains[3]. The pipe strain-meters A5 and A6 (A5', A6') were bent during the landslide activity caused by a typhoon in 1980. Therefore test boring (A5, A6) were made again at about 1 meter to 2 meters apart from the former pipe strain-meters (A5', A6'). As is clear from these figures, the slip surface exists at a depth of around
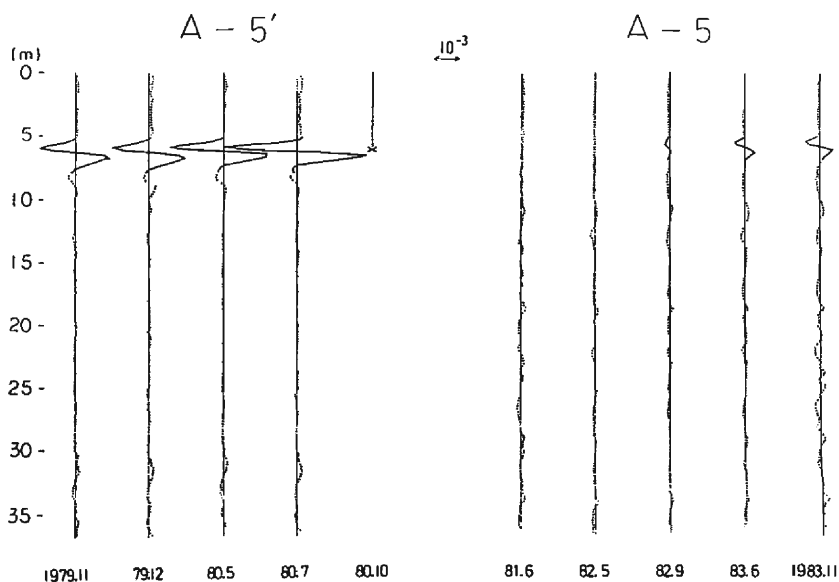
Fig. 3 (a). Values measured with an insert type of strain meter at site A5 in Fig. 2.
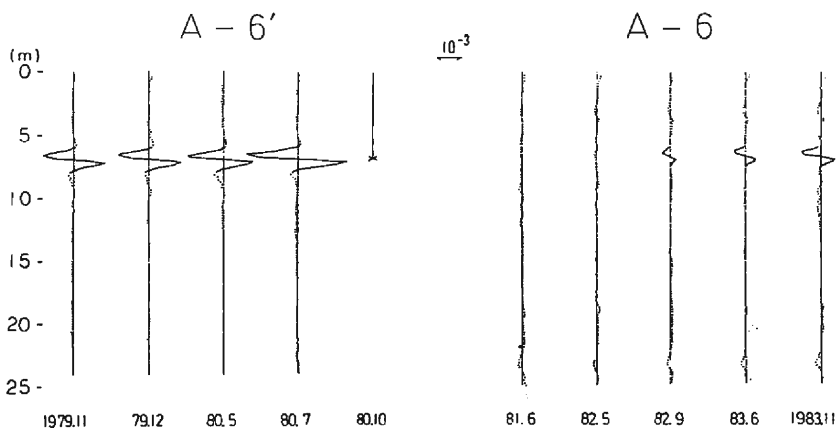

Fig. 3 (b). Values measured with an insert type of strain meter at site A6 in Fig. 2.

6.5 meters near A5 and around 7 meters near A6, respectively. The form of the ground surface was determined by topographic leveling prior to the landslide movement in 1980. The forms and positions of cracks at both sides of the landslide area could be determined on the ground surface. Consequently, the shapes of ground surface and slip surface in this case may be considered as known conditions of the boundary surfaces.

3.2 2-D Finite Element Method

It is difficult to express the deformation of slip surface by using a normal F.E.M.,

because the deformation of slip surface is large and the strength of slip surface shows elasto-plasticity, moreover a separation at slip surface may have taken place. In view of this situation, the author applied the 2-D F. E. M. supplemented by joint elements as introduced by Goodman[16] as a means for simulation and attempted to explain the observed landslide process quantitatively using this method.

Figure 4 shows the joint element constructed from four nodal points I, J, K and L. Two pairs of nodal points I-L and J-K are assumed to occupy the same coordinate in the initial state, that is, the surfaces I-J and K-L are in contact. Slip-surface behavior is expressed by the relative position of both surfaces of the joint element. The relative motion of both surfaces is classified as follows :

(i) parallel motion to the joint

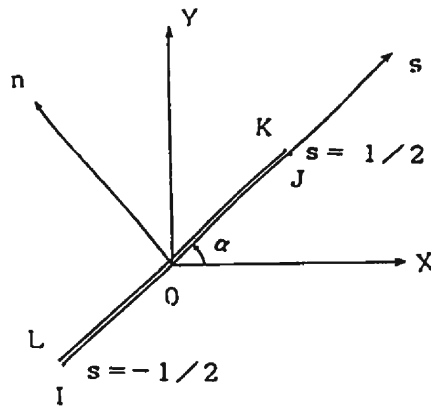(ii) perpendicular motion to the joint (open and contact)
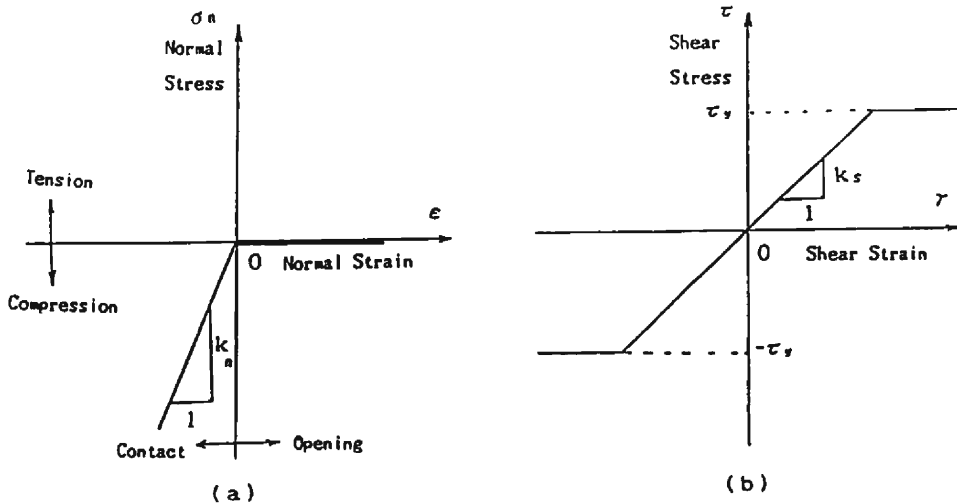

Fig. 4. Configuration of the joint element.

Fig. 5. Constitutive relationship for the joint element: (a) normal direction ; (b) shear direction.

(iii) rotational motion around the center of the joint element.

The deformation characteristics of the joint element are determined by the shear stiffness k_s, the normal stiffness k_n and the rotational stiffness k_ω. Since k_ω is a function of k_n, the constitutive relation of the joint element is expressed by two parameters k_s and k_n, as shown in **Fig. 5**[16),17)]. The yield shear stress, τ_y, is given by a function of the effective normal stress by assuming the Mohr-Coulomb's failure criterion.

$$\tau_y = c + \sigma'_n \ \tan\phi \quad \varepsilon < = 0$$
$$\tau_y = 0 \qquad\qquad \varepsilon > 0$$

in which c is the cohesion of the soil, σ'_n is the effective normal stress and ϕ is the internal friction angle.

In the present analysis by the F. E. M. the load-transfer method[16)] is employed. This method needs only a very short calculation time, because the stiffness matrix need be solved only once. The boundary conditions of external forces (pore-water pressures) are varied in 5 stages and calculations under each boundary condition are iterated until the stresses will be judged to converge with predecided criterion.

3.3 Analytical Condition

Figure 6 shows the cross section of slope and the arrangement of the joint elements on the slip surface to be analyzed by the F. E. M. The joint elements are arranged only along the slip surface. It is assumed that the strength of a slip surface is residual one, because landslide movement occurs along the same slip surface almost every year. The author assumes that the joint elements are devised so as to express the shear stress following the Mohr-Coulomb's failure criterion and that the normal stress is not transmitted across a joint once the joint element has been opened by tensile stress (see **Fig. 5**).

The soil is generally anisotropic. However, in the present landslide area, observations have proved it to be practically isotropic. The results of seismic survey for instance revealed a small difference between velocities in cross sections as well as in longitudinal sections at intersect points implying a weak anisotropy, but the soil is assumed to be isotropic because the differences were small. Density, cohesion and internal friction angle have been determined by soil test including triaxial tests under $\overline{CU}$ condition for core samples obtained from boreholes[14),15)]. It is assumed that the soil above the slip surface is linearly elastic. The soil is denoted by an isoparametric element[18)].

The boundary conditions are given as follows. The part below the joint elements are assumed to be fixed, because landslide movement occurs along the same slip surface almost every year. The displacement on the ground surface is kept free.

The problem remains unsolved as to the accuracy of the elastic constants of the soil mass and joints used in the F. E. M. The data available at this moment are those of P-wave velocity ($V_p = 800$ m/sec), density, cohesion and internal friction angle. S-wave velocity (V_s) can be inferred from the data on P-wave velocity assuming that $V_p/V_s = 2$. This ratio corresponds to Poisson's ratio being 0.35, and this value is probably reasonable considering the deep weathering found through boring-core observations.
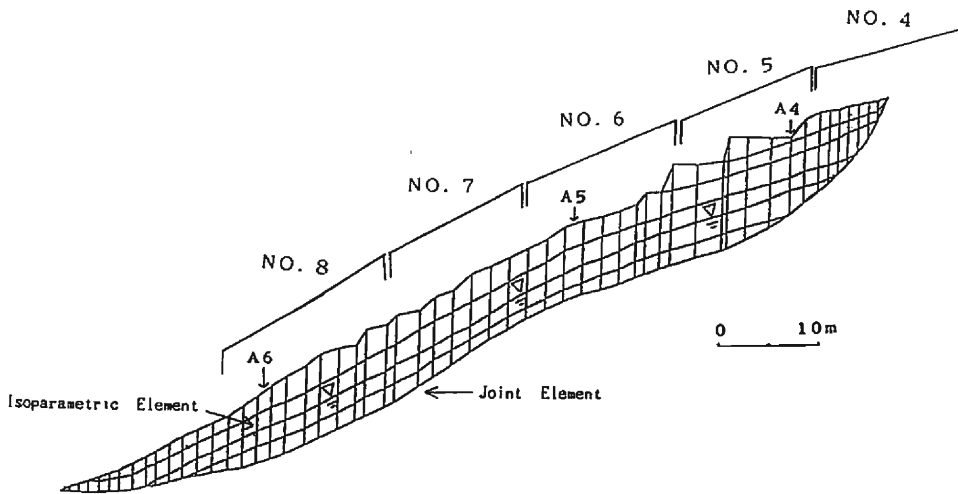
Fig. 6. Division of slope into finite elements. Joint elements are distributed only along the potential slip surface. The observed ground water level is indicated by ▽. The extensometer is indicated by ⌐¬.

Table 2 (a). Physical constants of isoparametric elements; Element No 1 is unsaturated soil, element No 2 is saturated soil

ISOPAMETRIC ELEMENT			
Number of element	Unit weight	Young's modulus	Poisson's ratio
1	2. 2t/m³	54500t/m²	0. 35
2	2. 3	57000	0. 35

Table 2 (b). Physical constants of joint elements

JOINT ELEMENT			
Cohesion	Stiffness of shear direction	Stiffness of normal direction	Internal friction angle
0. 07t/m²	1500t/m³	20200t/m³	30°

The normal stiffness of the joint element is calculated from S–wave velocity and Poisson's ratio, while the shear stiffness is assumed to be about 7. 5 percent of normal stiffness. The physical constants used for the present analysis are shown in **Table 2.**

All elements are subject to gravity. This force changes the shape of the elements and the distribution of stresses in the soil mass. The analyzed slope has no groundwater usually in the soil mass above the slip surface. This is taken to be the initial condition for self–weight analysis. Next, the pore–water pressures were applied to the upward direction, perpendicularly at the concerned joint elements. The pore–water pressure was assumed to be equal to the observed groundwater above the slip surface. The magnitude of these pressure were assumed to correspond to five different levels;

0. 25, 0. 5, 0. 75, 1. 0, or 1. 25 times the groundwater level observed during the outbreak of the landslide caused by the downpour in 1980. Since the groundwater level during landslide movement had been measured only once a day, it is quite possible that the groundwater level during the rupture exceeded the observed level. The groundwater level, equivalent to 25 percent of the observed level, corresponds to about one meter. Moreover, the change in groundwater level (A5) observed at the landslide movement in 1980 exceeded 6. 5 meters[15]. For this reason, an assumed value would be reasonable. Since the joint elements are defined by the Mohr-Coulomb's failure criterion, the increase in pore-water pressure has an effect to weaken the strength of joint elements. Therefore if the pore-water pressure is raised to a certain value, a landslide would be triggered.

In this analysis, a coupling problem between soil displacement and water pressure (stress-flow coupling problem) is ignored. Seepage pressures acting on the slip surface and soil particles are also ignored because there are no data for the analysis. The observed groundwater level was that in the borehole where strainers had been perforated at all depth. There is some doubt therefore if the observed groundwater level corresponds to the actual pore-water pressure acting on the slip surface. However, it is a fact that the slide was actuated while the groundwater level was high, and also it seems to be reasonable that the pore-water pressure and groundwater level are in close correlation. Thus, in the present analyses the pore-water pressure is assumed to correspond to that due to observed groundwater level.

4. Analytical Results

First, the ratio between the shear stress and the shear resistance for each joint element was calculated to determine a local factor of safety (L. F. S.) of i-th element as follows.

$$\mathrm{L.\,F.\,S.}_{i} = \frac{(c + \sigma'_i \tan\phi) \cdot l_i}{\tau_i \cdot l_i}$$

in which τ_i is shear stress, c is cohesion, σ'_i is effective normal stress, l_i is length of joint and ϕ is internal friction angle. The local factors of safety were calculated for every six case for self-weight and the five pore-water pressures. Since the displacements itself is resisted by neighboring element and remains small, it is assumed that the residual strength is maintained even if a slight movement occurs at places with the local factor of safety less than 1. Next, the total factor of safety is calculated to determine the whole stability. The total factor of safety (F. S.) is calculated as follows.

$$\mathrm{F.\,S.} = \frac{|\sum s_i \cdot l_i|}{|\sum \tau_i \cdot l_i|}, \quad |s_i| = c + \sigma'_i \tan\phi$$

The results of self-weight analysis are shown in the upper inset of **Fig. 7.** The shaded areas denote joint elements with a local factor of safety less than 1. They exist on both ends of the slip surface. The joint elements in the upper part of the slope were opened because the lower nodal points of the joint elements were fixed. These

Fig. 7.   Analytical results by F. E. M.   The shaded areas denote joint elements with a local factor of safety less than 1.   F. S. shows a total factor of safety; (a), (b) and (c) correspond to self weight, 0. 25 and 0. 50 time the observed gcoundwater level, respectively.
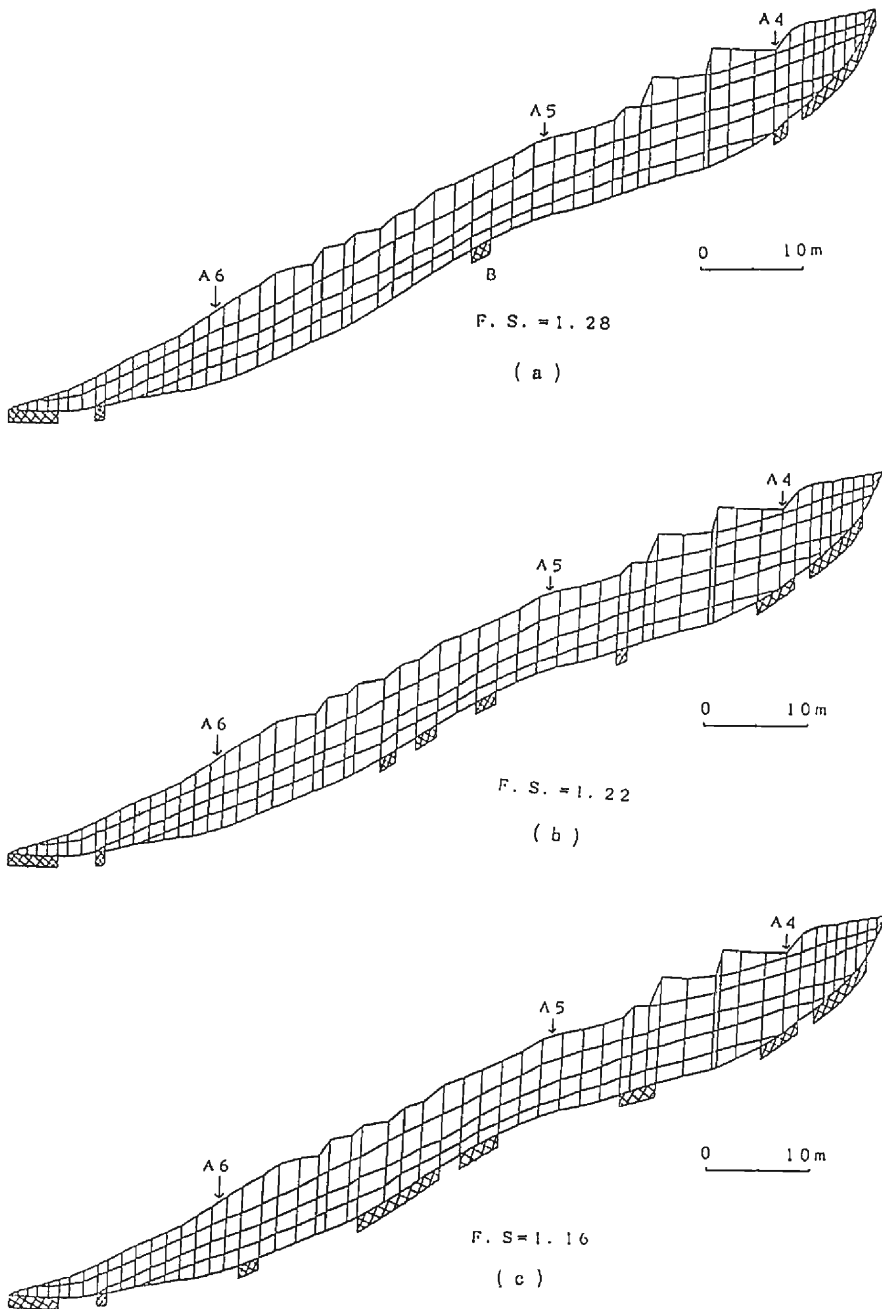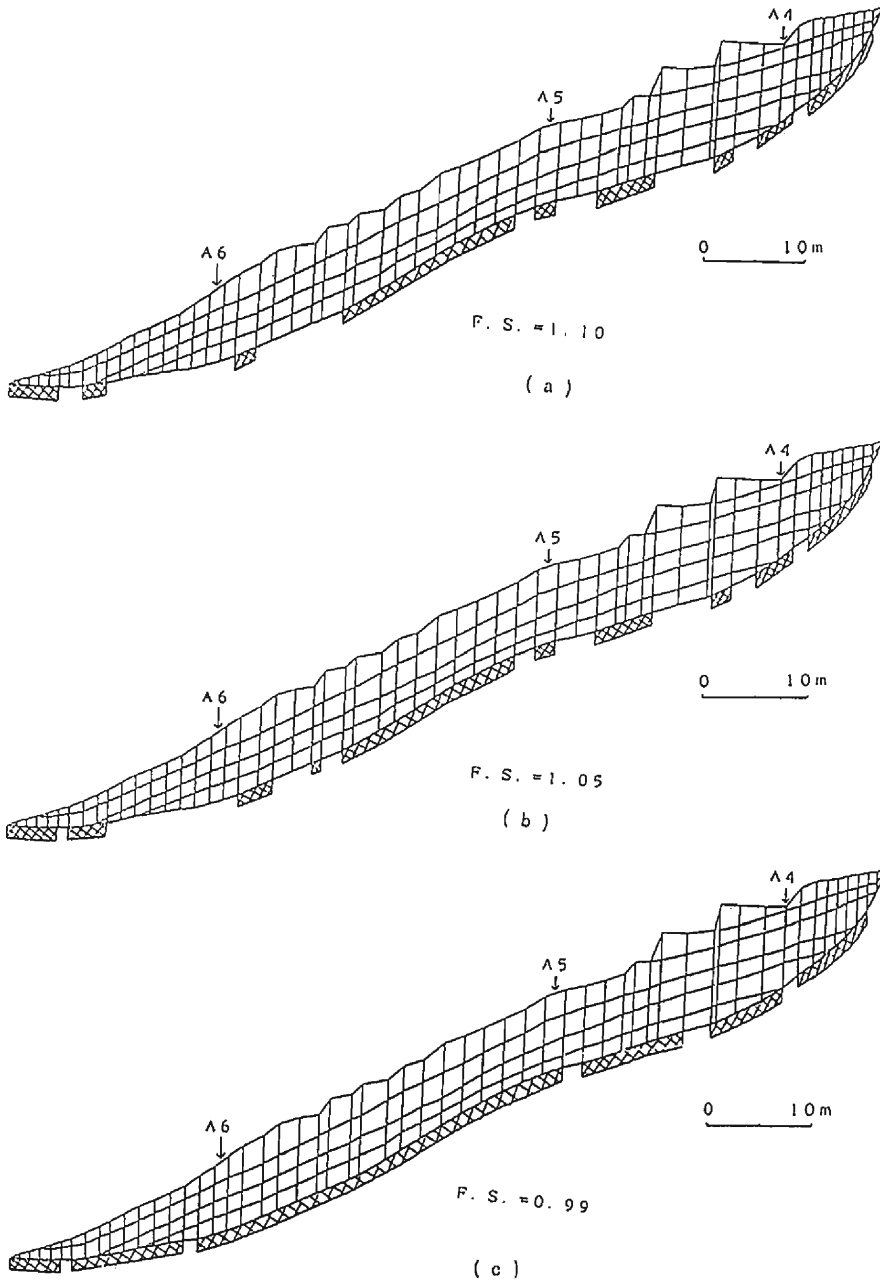
Fig. 8. Analytical results by F. E. M. The shaded areas denote joint elements with a
local factor of safety less than 1. F. S. shows a total factor of safety; (a), (b)
and (c) correspond to 0. 75, 1. 0 and 1. 25 times the observed groundwater
level, respectively.

gave an aggravating influence upon the local facter of safety in the upper part of the slope. This is a probable reason for the local factor of safety less than 1 in the upper part of the slope. In the lower part of the slope, little shear stress and thus little displacement was induced by the accumulated residual shear stress of the upper slope. This is supposed by the cause for the local factor of safety less than 1 in the lower part of the slope. But the total factor of safety still remained 1.28.

The middle inset of **Fig. 7** shows the case when 25 percent of the observed groudwater level acts on the joint elements as pore-water pressure and the total factor of safety is 1.22. The case for 50 percent of groundwater level is shown in lower inset of **Fig. 7** where the total factor of safety is 1.16. The case for 75 percent of groundwater level is shown in the upper inset of **Fig. 8** where the total factor of safety is 1.10. The middle inset of **Fig. 8** shows the case when the pore-water pressure corresponds to the observed groundwater level and the total factor of safety is 1.05. Thus, even in this case the slope does not slide yet as a whole. However, at a number of areas a local factor of safety has already decreased to less than 1. The lower inset of **Fig. 8** shows the case where the pore-water pressure was 1.25 times the observed groundwater level. In this case, the displacement grows too large to maintain the equilibrium necessary for an analysis by the F. E. M. In other words the solution does not converge any more and thus computation is forced to stop. The displacement of each nodal point increased. The total factor of safety in this case was 0.99 and it reflects to the instability of the slope as a whole.

5. Discussion

Figure 9 shows the local factor of safety under self-weight and five different pore-
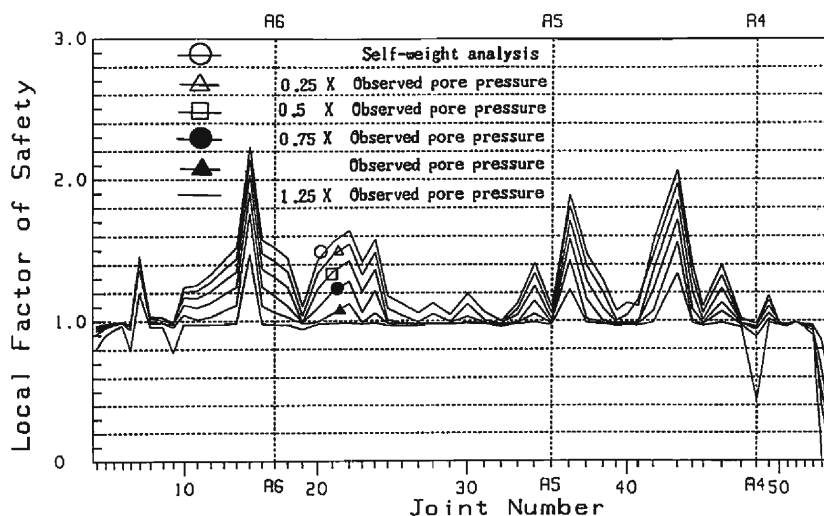
Fig. 9. The local factor of safety under the condition of self-weight and five different pore-water pressures corresponding to 0.25, 0.5, 0.75, 1.0 and 1.25 times the observed groundwater level.

water pressures ; corresponding to 0.25, 0.5, 0.75, 1.0 or 1.25 times the observed groundwater level. The highest value for the local factor of safety is obtained in the case of self-weight analysis, while the factors become smaller in order of the pore-water pressure, 0.25, 0.5, 0.75, 1.0 and 1.25. In the case when the pore-water pressure corresponds to 1.25 times the observed groundwater level, the shear stresses of all the joints between A5 and A6 reach the yield stresses and shear failure takes place.
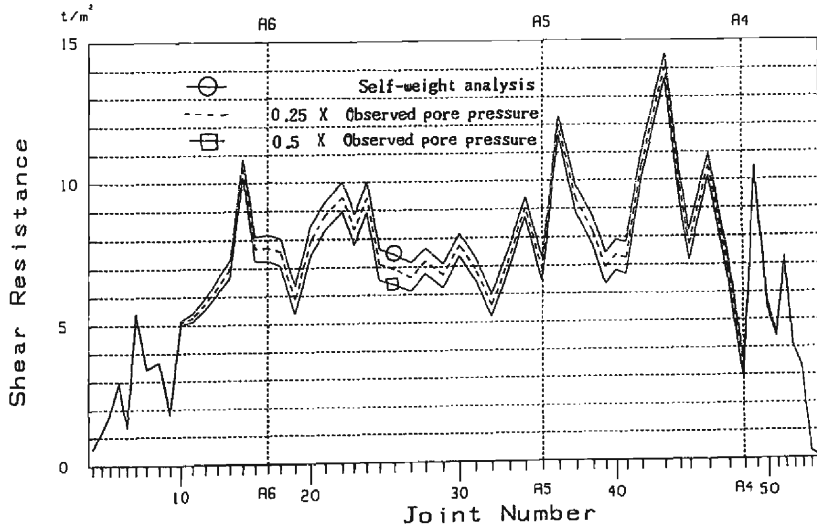

Fig. 10 (a).   The shear resistance of the joint elements under the condition of self-weight, 0.25 and 0.5 time the observed groundwater level.

Fig. 10 (b).   The shear resistance of the joint elements under the condition of 0.75, 1.0 and 1.25 times the observed groundwater level.

The shear resistance acting on every joint for each condition is shown in **Fig. 10** (a) and **Fig. 10(b)**. The highest value for shear resistance is obtained in the case of self-weight analysis, while the shear resistance becomes smaller in order of the pore-water pressure, 0. 25, 0. 5, 0. 75, 1. 0 and 1. 25 on the whole. Consequently this procedure for pore pressure is reasonable. Some of the values at both ends of the slope for 1. 25-times the groundwater level exceed the value of other conditions. This is likely influenced

Fig. 11 (a). The shear stress of the joint elements under the condition of self-weight, 0. 25 and 0. 5 time the observed groundwater level.

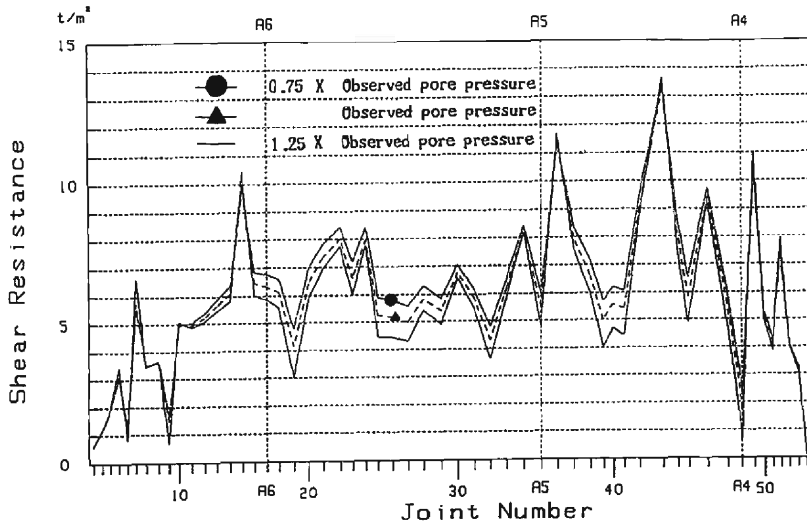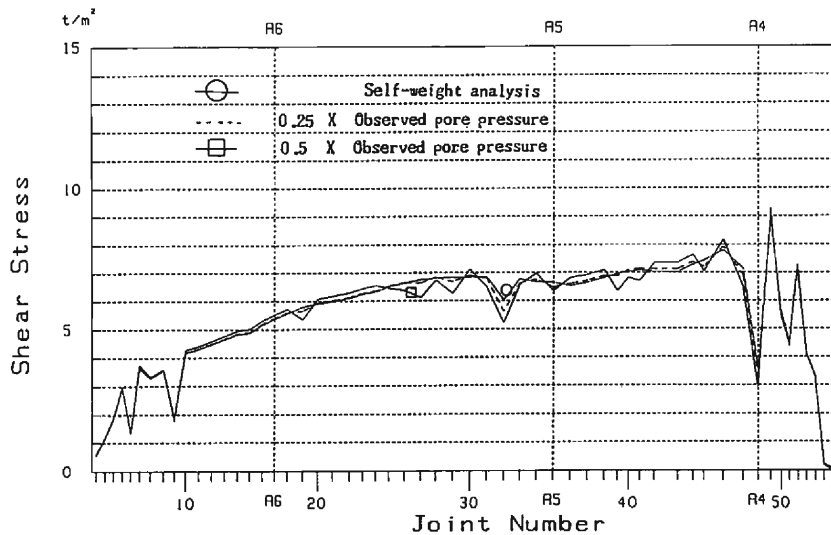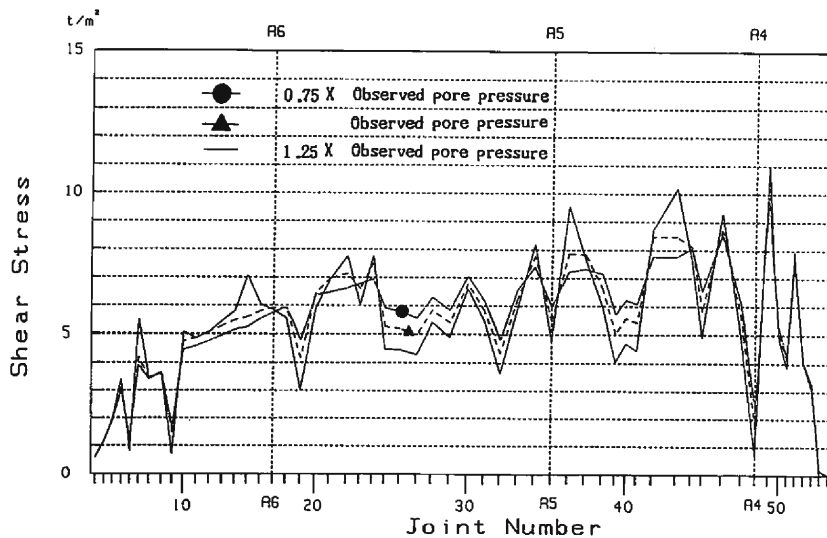Fig. 11 (b). The shear stress of the joint elements under the condition of 0. 75, 1. 0 and 1. 25 times the observed groundwater level.

by the forced stopping of the iteration calculation. Except for these values, the results seem reasonable.

The shear stress that acts on every joint for each condition is shown in **Fig. 11(a)** and **Fig. 11(b)**. As is clear from the figures, the shear stress in self-weight analysis and those in the cases for 0.25 and 0.5 time the observed groundwater level are rather uniform. When the pore-water pressures are 0.75, 1.0 and 1.25, the shear stress at every point fluctuates greatly. The shear stress acting at each joint between A5 and A6, especially those at joints 22, 24 and 34, becomes larger as the pore-water pressure increases. In addition, since the local factor of safety at these joints decreases gradually, it is considered that the condition during actual landslide is well reproduced (see **Fig. 9**).

Measurements by extensometers for the ground surface show that the spans of the extensometer No. 4, No. 5 and No. 6 are in extension, while the spans for No. 7 and No. 8 are in compression (see **Fig. 2** and **Fig. 6**)[15]. The analytical results of the F. E. M., when pore-water pressure corresponding to 1.25 times the observed groundwater level is exerted, show that all the spans for the ground surface over the joints No. 1 to No. 31 are in compression, while the spans for the ground surface over the joints No. 32 to No. 56 are in extension (see **Table 3**). These simulated results are in good agreement with the observed facts.

Next, let us examine the local factors of the areas around the pipe strain-meters of A5 and A6. A comparison between **Fig. 7** and **Fig. 9** shows the following ; The third joint element downward from A5 (B in **Fig. 7**) has a local factor of safety less 1 when analyzed for self-weight. The area between A5 and A6 has a local factor of safety less than 1 when analyzed for 0.25 time the groundwater level. The area of local factors of safety less than 1 is enlarged when the pressure is 0.5 time. Further, the local factor of safety of A5 is less than 1 when the pressure is equivalent to 0.75 time the observed groundwater level, while that of A6 still remains over 1. However, all the

Table 3. Calculated strain at ground surface ; No is the number of isoparametic elements at ground surface ; Positive value implies extension and negative value compression

No	Strain	No	Strain	No	Strain	No	Strain	No	Strain
1	0.0	2	0.0	3	$-0.822E-5$	4	$-0.106E-4$	5	$-0.106E-4$
6	$-0.128E-4$	7	$-0.403E-4$	8	$-0.369E-4$	9	$-0.486E-4$	10	$-0.275E-4$
11	$-0.191E-4$	12	$-0.167E-4$	13	$-0.729E-5$	14	$-0.242E-4$	15	$-0.261E-4$
16	$-0.259E-4$	17	$-0.441E-4$	18	$-0.349E-4$	19	$-0.303E-4$	20	$-0.159E-4$
21	$-0.274E-4$	22	$-0.150E-4$	23	$-0.273E-4$	24	$-0.125E-4$	25	$-0.310E-4$
26	$-0.286E-4$	27	$-0.265E-4$	28	$-0.275E-4$	29	$-0.131E-4$	30	$-0.142E-4$
31	$-0.104E-4$	32	$0.870E-6$	33	$0.107E-4$	34	$0.196E-4$	35	$0.329E-4$
36	$0.213E-4$	37	$0.283E-4$	38	$0.149E-4$	39	$0.189E-4$	40	$0.216E-4$
41	$0.146E-4$	42	0.0	43	$0.384E-4$	44	$0.337E-5$	45	$0.477E-6$
46	$0.801E-5$	47	$0.571E-5$	48	$0.315E-5$	49	$0.561E-5$	50	$0.122E-4$
51	$0.935E-5$	52	$0.639E-5$	53	$0.187E-5$	54	$0.731E-5$	55	0.0
56	$0.443E-5$								

joints between A5 and A6 have a local factor of safety less than 1 when the pore-water pressure is equivalent to 1.25-times observed groundwater level. This simulation suggests that the nucleus of the landslide was between A5 and A6, a point near A5, and the rupture developed bilaterally along the slope, i.e. the local factor of safety for the area around A5 became less than 1 first, and then that for the area around A6 followed.

It is impossible to confirm the exact position of the nucleus of the failure, because there was no pipe strain-meter between A5 and A6. But the extensometer No.6 close to the pipe strain-meter A5 showed the largest extension measured in this event. The lower pile of the extensometer, immediately next to A5, toppled over due to a large movement and as a consequence the total displacement of the slope could not be measured. The toppling at this position suggests that this area moved most actively among all other areas during the landslide movement in 1980. It is probable therefore that this area is the starting point of the landslide. If it is the case, the rupture started around A5 and reached the instrument A5 first and enlarged down the slope. The simulation given in the preceding section agrees with the observed fact by using the extensometers, that is, landslide movement occurred around A5.

The simulation suggests that the sliding proceeded with the rise and fall of pore-water pressure. If the period of duration betweeh the 0.75 time and the 1.25 times the observed groundwater level were about ten hours, an average rate of the rupture process would be harmonized with the observed process, because the distance between A5 and A6 is about 30 meters.

After the landslide had ceased and stabilized, the pore-water pressur of the areas around A5 and A6 has been continuously measured in boreholes. It has been found
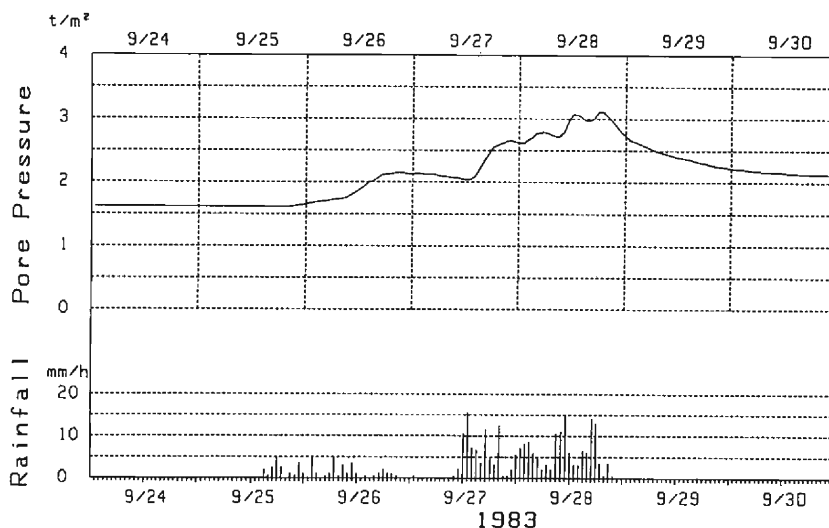
Fig. 12. An example of observation of pore-water pressure at site A6 in Fig. 2. Strainers have been perforated from 6 to 7 meters.

that the pore-water pressure has reached a peak with in about 10 to 30 hours after a rainfall, where the delay time calculated from the observation result shown in **Fig. 12.** As mentioned before, an enlargement of the rupture, from A5 to A6, can be explained by an enlargement of the area where a local factor of safety is less than 1. If it is the case, the progression velocity of the rupture agrees with the rate of increase in pore-water pressure. It is therefore reasonable that the increased duration of the pore-water pressure on the slip surface can be taken to be of the order of about ten hours. In that case, the results of analyses, in a gross manner, explain the observed results on the progression velocity of the rupture which is a few meters per hour, as estimated from the difference of arrival times of movement in the order of A5 to A6.

6. Conclusion

The main physical characteristics of a landslide mechanism have been determined through observations by the pipe strain-meters and extensometers along line A at the Irahara landslide area Tokushima Prefecture during the landslide caused by a rainfall of more than 570 millimeters over a few days in September 1980. A rupture started at a point on the slip surface near the pipe strain-meter A5, while the soil above the slip surface was elastic. The rupture progressed downhill from A5 to A6 along the slope at an average velocity of a few meters per hour. The mechanism of this progression of rupture zone along the slip surface is interpreted by the enlargement of local failure accompanied by the increase in the pore-water pressure, which was simulated by the F. E. M. with the joint elements along the slip surface. From this analysis, it is pointed out that the progression of the rupture has been controlled essentially by rise and fall of the pore-water pressure accompanying the rainfall during the slide.

References

1) Suemine, A. : Observational Study on Landslide Mechanism in the Area of Crystalline Schist (Part 1) –An Example of Propagation of Rankine State, Bull. Disas. Prev. Res. Inst., Kyoto Univ., Vol. 33, Part 3, 1983, pp. 105-127.

2) Suemine, A. and M. Shima : Monitoring of Propagation of Subsurface Deformation in a Crystalline-Schist Landslide, INTEPRAVENT 1984, VILLACH, Vol. 2, pp. 49-60.

3) Shima, M. and A. Takeuchi : On a Method of Instrumentation of Underground Deformation, Landslides, Journal of Japan Landslide Society, Vol. 10, No. 2, 1973, pp. 6-17 (in Japanese).

4) Suemine, A., M. Shima and T. Konishi : Slip Surface in some Crystalline-Schist Landslides, Proc. of 23rd Annual Conf. of Japan Landslide Society, 1984, pp. 72-75 (in Japanese).

5) JSSMFE : Handbook of Soil Mechanics and Foundation Engineering, 1972, pp. 225 (in Japanese).

6) Morgenstern, N. and Price, V. E. : The Analysis of the Stability of General Slip Surfaces, Geotechnique, Vol. 15, No. 1, 1965, pp. 79-93.

7) Spencer, E. : A Method of Analysis of the Stability of Embankment Assuming Parallel Inter-Slice Forces, Geotechnique, Vol. 17, No. 1, 1967, pp. 11-26.

8) Janbu, N : Application of Composite Slip Surface for Stability Analysis, Proc. European Conf. on Stability of Earth Slope, Vol. 3, 1954, pp. 43-49.

9) Bishop, A. W. : The use of the Slip Circle in the Stability Analysis of Slopes, Geotechnique, Vol. 5, No. 1, 1955, pp. 7-17.

10) Nomitsu, T. : Landslide, TIKYUBUTURI, No. 1, 1942, pp. 135-152 (in Japanese).

11) Kitahara, Y. : Some Consideration on Stability Problems of excavated Slopes, Tsuchi-to-Kiso, JSSMFE, No. 244, Vol. 26, 1978, pp. 23-30 (in Japanese).

12) Lo, K. Y. and Lee, C. F. : Stress Analysis and Slope Stability in Strain-Softening Materials, Geotechnique, Vol. 23, No. 1, 1973, pp. 1-11.

13) Hada, M., T. Ishii, T. Kawai and N. Takeuchi : Limit Analysis of a Locally Submerged Slope by means of Kawai Models, Proc. of 17th Japan Conf. on Soil Mechanics and Foundation Engineering, 1983, pp. 1101-1104 (in Japanese).

14) Shima, M., Y. Kobayashi, A. Suemine, A. Nakagawa and T. Konishi : The Investigation Report at Irahara Landslide, Disas. Prev. Res. Associ., 1980 (in Japanese).

15) Shima, M., A. Suemine, and T. Konishi : The Investigation Report at Irahara Landslide, Disas. Prev. Res. Associ., 1981 (in Japanese).

16) Goodman R. E. : Methods of Geological Engineering in Discontinuous Rocks, West Publishing Co., St. Paul, 1976, pp. 300-368.

17) Toki, K., T. Sato and F. Miura : Separation and Sliding between Soil and Structure during strong Ground Motion, Earthquake Engineering and Structural Dynamics, Vol. 9, 1981, pp. 263-277.

18) Zienkiewicz, O. C. : The Finite Element Method in Engineering Science, McGraw-Hill House, 1971. (Translation published by BAIFUKAN Co.).

Appendix

Table 1. List of correspondence of internal strain meter

Internal strain meter Part 1	Internal strain meter Part 2
No. 1	A-3
No. 2	A-4
No. 3	A-5
No. 4	A-6
No. 5	A-7
No. 6	A-8
No. 7	A-1
No. 8	A-2
No. 9	B-3
No. 10	B-5
No. 11	B-6
No. 12	B-7
	B-1
	B-2
	B-4

ERRATUM

Observational Study on Landslide Mechanism in the Area of Crystalline Schist (Part1) –An Example of Propagation of Rankine State

By Akira Suemine

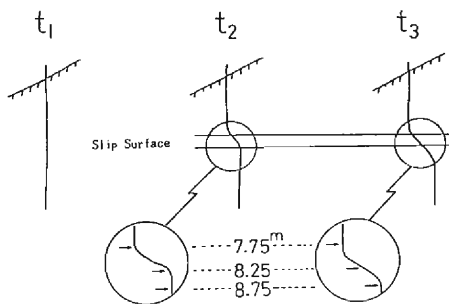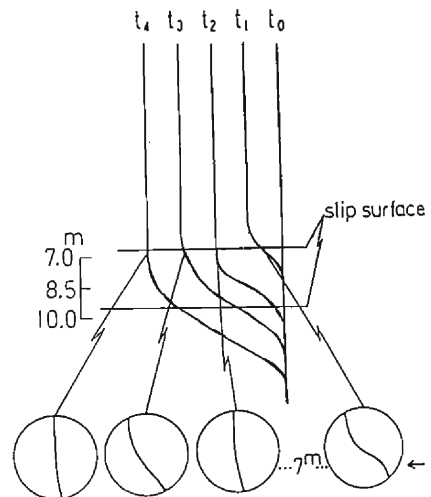Figure 5 and Fig. 17 in Part 1 should be changed next figures.

Fig. 5

Fig. 17